ELSEVIER

Journal of Chromatography A, 695 (1995) 165–174

JOURNAL OF CHROMATOGRAPHY A

Near-infrared laser-induced fluorescence detection in column liquid chromatography. A comparison of various lasers and detection systems
I☆. Continuous wave lasers

A.J.G. Mank*, N.H. Velthorst, U.A.Th. Brinkman, C. Gooijer

Department of General and Analytical Chemistry, Free University, De Boelelaan 1083, 1081 HV Amsterdam, Netherlands

First received 21 June 1994; revised manuscript received 2 December 1994

Abstract

Several lasers, i.e. HeNe lasers, diode lasers and an argon-ion–dye laser combination, are compared as excitation sources for near-infrared laser-induced fluorescence detection in column liquid chromatography. Using a model gradient liquid chromatography system, detection limits for disulphonated aluminum phthalocyanine (AlPcS2) were compared after optimization of the signal processing scheme for each laser. The best detection limit ($1.5 \cdot 10^{-13}$ *M*) was obtained for the argon-ion–dye laser combination, applying ratioing of emission and excitation light to reduce flicker noise. Utilizing diode laser excitation there is no need for ratioing so that emission collection can be improved and a detection limit similar to that obtained with the argon-ion laser can be achieved. As this device is very cheap, the diode laser is the best choice for most applications. If tunability over a large wavelength region is essential, the argon-ion–dye laser combination is a good but expensive alternative.

1. Introduction

Recently, much attention has been paid to the development of laser-induced near-infrared fluorescence methods for detection purposes in, for instance, conventional-size column liquid chromatography (LC). Compared with conventional helium–cadmium or argon-ion laser-induced fluorescence (LIF) [1], detection in the near-infrared (NIR) has some obvious advantages. First of all, cheap and stable helium–neon (HeNe) lasers and diode lasers can be used for excitation. Furthermore, background fluorescence intensity is low, Raman scatter is weak (proportional to λ^{-4}) and photochemical decomposition is negligible. On the other hand, the number of analytes that can be detected without chemical derivatization is limited; this explains the recent attention directed to the development of covalent-labelling procedures with NIR-absorbing fluorophores [2]. Still, photosensitizers (like phthalocyanines) used in photodynamic therapy form a very interesting and relevant group of compounds that can be excited directly [3].

In the present study the performance of the various lasers as excitation sources in NIR LIF detection after LC is examined. Part I is devoted

* Corresponding author.

☆ For Part II see Ref. [16].

0021-9673/95/$09.50
SSDI 0021-9673(94)01195-8

Table 1
Spectroscopic characteristics of several near-infrared lasers

Laser type	Wavelength (nm)	Pulsed/CW	Power (mW)[a]	Fluctuation (%)[b]
HeNe	633	CW	2–15	0.1–0.5
Diode	630–690	CW	3–30	0.1–0.5 (0.0025)
Argon-ion	Several lines[c]	CW	100[d]	0.5–3 (0.05)
Nd:YAG	1064/532/355[c]	Pulsed	20 000/6/10[d]	10–30 pulse-to-pulse
XeCl-excimer	308[c]	Pulsed	10 000/15/100[d]	2–3 pulse-to-pulse

[a] Peak power/pulse duration (ns)/repetition rate (Hz).
[b] Value between parentheses can be achieved with feedback stabilization.
[c] Indicates the need of a dye laser to obtain red or NIR laserlight.
[d] Laser dyes used: Rhodamine 101 (22% efficiency for argon-ion laser excitation), Oxazine 170 (20% efficiency for Nd:YAG laser excitation) and DCM (12% efficiency for XeCl-excimer laser excitation).

to continuous wave (CW) lasers, i.e. various diode and HeNe lasers as well as a tunable argon-ion–dye laser combination. Part II deals with the performance of readily tunable pulsed lasers (which are not often applied for LC–LIF detection), i.e. a frequency-doubled Nd:YAG laser and an excimer laser, both combined with dye lasers. Some general characteristics and spectroscopic features are presented in Table 1 [4].

Gradient LC of a mixture of disulphonated aluminum phthalocyanine (AlPcS2) isomers, containing 85% of one isomer, is used as a model LC system [5]. This mixture is considered one of the most relevant photosensitizers available for photodynamic therapy and was introduced only recently. Chromatographic separation of the various AlPcS2 isomers is necessary, because their spectroscopic properties are very similar and they are expected to show both different effectivity as photosensitizers and different retention mechanisms in the body [5].

2. Experimental

2.1 Chemicals

HPLC-grade methanol was purchased from J.T. Baker Chemicals (Deventer, The Netherlands). Purified disulphonated aluminum phthalocyanine (AlPcS2), synthesized by direct sulphonation of non-substituted AlPcCl and fractionated by reversed-phase (RP) LC, was obtained from Porphyrin Products (Logan, UT, USA). All laser dyes were obtained from Radiant Dyes (Wermelskirchen, Germany).

2.2 Chromatography

The degassed eluent was delivered by two Applied Biosystems (Foster Hill, CA, USA) Series 400 pumps, controlled by the computer of a 1000 S diode array detector. A Valco injection valve equipped with a 25-μl loop was used for sample injection on a 250×3.1 mm I.D. C_{18} (5-μm particles) Vydac (Hersperia, CA, USA) analytical column. A 10×3.0 mm I.D. C_{18} (20-μm particles) home-made precolumn was used to protect the analytical column. Linear gradient elution was performed from methanol–5 m*M* phosphate buffer (pH 4.0) (25:75, v/v) to methanol–5 m*M* phosphate buffer (pH 4.0) (90:10, v/v) in 15 min, at a flow rate of 1.0 ml min^{-1}, followed by a further 10 min isocratic elution.

2.3 Detection

Information about detection and signal processing instrumentation used and, if relevant, its optimization is given below.

General

The absorption spectrum of AlPcS2 was recorded on a DU-64 spectrophotometer (Beckman, Anaheim, CA, USA). The fluorescence spectra were recorded on a LS-50 spectrofluori-

meter (Perkin Elmer, Gouda, The Netherlands) equipped with a R928 photomultiplier (PMT) (Hamamatsu Photonics, Hamamatsu City, Japan).

The absorption maxima of AlPcS2 (ϵ = 180 000 l mol^{-1} cm^{-1}) in methanol and water are at 670.4 nm and 671.6 nm, respectively. The emission maxima are found at 678.0 nm and 680.0 nm, with corresponding fluorescence quantum efficiencies of 0.50 and 0.37, and fluorescence lifetimes of 6.2 ns and 5.1 ns, respectively [6]. Triplet state yields of 0.3–0.4 in water and methanol have been reported for several sulphonated phthalocyanines, with triplet state lifetimes of 250–500 μs [7–9]. In this paper a fluorescence quantum yield of 0.43, a fluorescence lifetime of 6.0 ns, a triplet state quantum yield of 0.33 and a triplet state lifetime of 300 μs are assumed for AlPcS2 in the LC eluent [9].

Detector cell

On-line fluorescence detection is performed with a two-fiber detector cell (Fig. 1), based on a home-made quartz flow cell (Suprasil I) with external dimensions of 4.0 × 4.0 × 10 mm and an internal bore of 1.1 mm. Collection of the fluorescence light takes place via a 60 cm long quartz fiber (1.2 mm outer diameter; 1.0 mm core diameter) with a 0.22 numerical aperture (Quartz and Silice, Uithoorn, The Netherlands). The cladding is stripped over a length of 7 mm, starting from the distal end of the fiber, to allow insertion of the fiber into the bore of the flow cell. A similar fiber is inserted from the other side of the flow cell for the collection of a small amount of light, elastically scattered by the eluent, to create a reference signal that is linearly dependent on the laser intensity.

A collimated laser beam is directed through the flow cell perpendicular to the flow direction. The fluorescence light is guided through the fiber to an adjustable lens holder, focused onto a PMT through a 2.5 cm $f/\# = 1$ lens and a set of emission filters that will change with the light source. Focusing is necessary because of the relatively small active area of the PMT (7.6 × 23 mm, rectangular). After intensity reduction with neutral-density filters to avoid overloading, the reference signal is guided through the other fiber to a similar PMT.

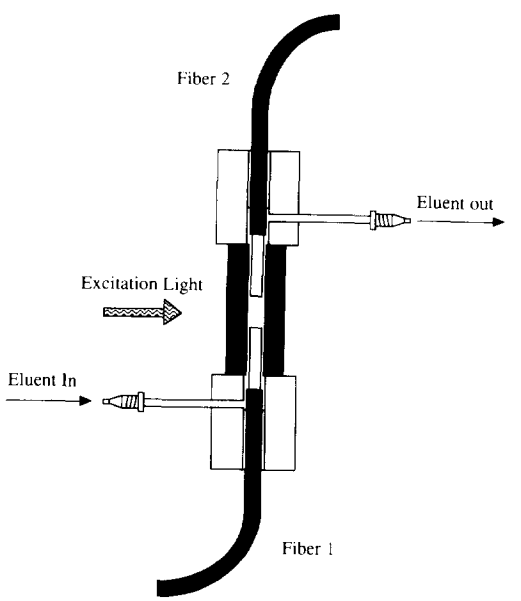

Fig. 1. Side view of the detector cell with two fibers put in from the top and the bottom, secured with fingertights; 1/16-in. LC connections are positioned perpendicular to the eluent stream through the flow cell.

Illuminated volume

The laser beam is collimated and adjusted to a beam diameter of 500 μm on entering the flow cell, using a number of lenses with different focal lengths. Apart from the diode lasers, the beam diameter was (500 ± 50) μm and gaussian in profile for all lasers tested. This corresponds to an illuminated volume of about 0.2 μl, which is small for conventional-size LC applications [10]. The beam emitted by diode lasers is elliptical, with a maximum "beam width" of (500 ± 50) μm and a maximum "beam height" of (190 ± 20) μm. The major axis is taken parallel to the fiber surface. Divergence of the excitation beam within the flow cell is limited to about 10 μm due to the small difference in refractive index between the LC eluent and the fused silica of the flow cell. A spatial filter (500 × 500 μm) is applied to remove any light emitted outside this region. Both fiber tips are positioned at 250 μm distance from the beam edge with home-made fingertights (Fig. 1).

Emission collection

Direct scatter from the flow cell and the fibers is negligible because of the spatial filter. The high reflections from the outer (air–fused silica) surface of the flow cell (4%) lie beyond the field of view of the fibers. Reflections on the inner (fused silica–eluent) surface are much lower in intensity ($<0.4\%$) as a result of the smaller difference in the refractive index. Long-pass emission filters are used to remove the remaining elastic scatter.

Fluorescence background from the flow cell and eluent impurities is of little influence in the NIR region. Raman scatter forms the most significant source of background, though it has a low intensity and stretches over a large wavelength region; for example, the strong Raman band of water lies beyond 840 nm for excitation at 670 nm. A LS-740 0.5″ short-pass filter (Corion, Holliston, MA, USA) is therefore used in all detection setups to remove much of the unwanted Raman scatter. The use of polarization filters to remove scattered excitation light did not reduce the background enough to compensate for the loss of transmitted fluorescence signal.

The emission collection filter set was optimized for each tested laser by adding combinations of 2–4 mm RG5, RG665, RG695 long-pass filters (Schott Nederland, Tiel, The Netherlands). In all cases the filters were sufficient to remove the elastically scattered laser light. The transmission of emission light through bandpass filters was found to be very low and therefore such filters were not used in the present study.

NIR detection

Several detectors are available for NIR detection, i.e. various types of photodiodes and PMTs. Simple (p–i–n) silicon photodiodes with an acceptable noise equivalent power (NEP) can be used ($15 \cdot 10^{-14}$ W $\sqrt{\text{Hz}^{-1}}$ at 700 nm for a 25 mm^2 sensitive area) in combination with integrated preamplifiers [11]. Silicon avalanche photodiodes show a 10-fold lower NEP and a quantum efficiency (QE) of 0.7–0.8 between 600 and 800 nm.

In this study C31034A02 GaAs PMTs (Burle, Lancaster, PA, USA) (QE = 0.25 at 700 nm) are used for all detection set-ups, because signal-to-noise (S/N) ratios were at least 20-fold higher for the PMT, compared to the photodiode–preamplifier combinations. The PMTs are operated at 1750 V with an EG & G Ortec (Oak Ridge, TN, USA) Model 456H high-voltage power supply and cooled to −23°C with a PMT housing from Products for Research (Danvers, MA, USA), regulated with a home-made controller. Fast electronics supplied by Products for Research provided a 2.5 ns rise time and 33 ns transit time for the PMT.

2.4 Signal processing

Three types of processing of the PMT signal were used, i.e. direct amplification, analog ratioing and photon counting.

Direct amplification

The PMT output is passed through a current-to-voltage converter, based on a AD515ALH operational amplifier (Analog Devices, Norwood, MA, USA) in combination with different feedback resistors and capacitors to scale the conversion factor (Fig. 2, dashed lines). After conversion, a 1 Hz second-order low-pass R × C filter is applied and the signal is either displayed directly on a Kipp and Zonen (Delft, The Netherlands) BD111 recorder or digitized using an Apple Macintosh SE computer.

Analog ratioing

Compared to digital ratioing after data collection, analog ratioing has the advantage that the rate at which the fluorescence and the reference signal are compared can be much higher. An analog ratioing system was built and optimized as described in ref. 1 (Fig. 2, solid lines). The heart of the system is an Analog Devices AD538 analog multiplier, configured in a single quadrant analog division mode.

The reference signal applied is much more intense than the fluorescence signal to reduce the influence of shot noise; by utilizing a smaller amplification factor, the resulting signals are

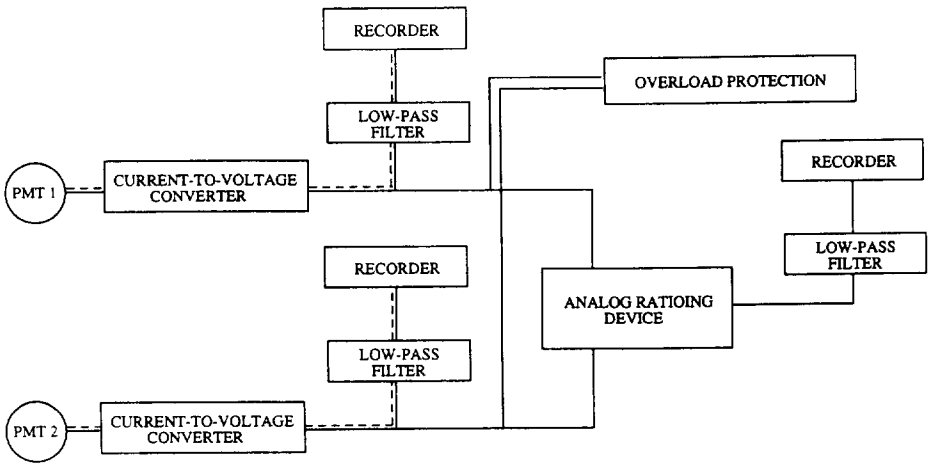

Fig. 2. Signal processing scheme. Dashed line = direct amplification; solid line = analog ratioing.

brought to the same intensity before ratioing is performed. Thus, under optimum conditions, ratioing allows detection limits to be determined by shot noise on the fluorescence signal.

Photon counting

Data from a SR400 photon counter (Stanford Research Systems, Palo Alto, CA, USA) are sent to an Apple Macintosh SE and handled in real time with a home-made programme that transforms the raw SR400 data into ASCII. Measurements can be performed using two detection channels at the same time, which allows ratioing after data collection.

The detection system was evaluated in terms of its "classic" photon counting performance [12]. For a PMT voltage of 1850 V, the dark current count rates were below 10 counts s^{-1} when using a photon counter threshold of −10 mV. At this PMT voltage nearly all photoelectron events induce a signal above the threshold, which is a prerequisite for photon counting since under shot noise-limited conditions photon counting is more sensitive than analog signal processing only if the discriminator coefficient is unity [13]. As the background rarely reached values below 1000 counts s^{-1}, dark current noise is negligible.

2.5 Laser systems

Two HeNe lasers, various types of diode lasers and an argon-ion–dye laser combination were tested.

HeNe lasers

The two lasers are HeNe(1): Spectra-Physics Model 117A (Mountain View, CA, USA), emitting 2 mW (TEM_{oo}); fluctuations in the output power are 0.1% for 1 min and 0.3% for 1 h, and HeNe(2): NEC (Tokyo, Japan) GLG5700/GLG5702 power supply, emitting 15 mW (TEM_{oo}); laser intensity instability, 0.2% for 1 min and 0.5% for 1 h.

Diode lasers

The operating characteristics of the diode lasers involved are given in Table 2. All diode lasers are biased by a LD2310 diode laser driver in combination with a AC9400 power supply (Seastar Optics, Seattle, WA, USA). Optical feedback is used to stabilize the diode lasers, which results in a maximum flicker noise of $8 \cdot 10^{-3}$% over 1 min and $1 \cdot 10^{-2}$% over 30 min. Applying a cheap LDD-200 driver unit (Meredith, Glendale, AZ, USA), which also uses an optical feedback loop, resulted in a short-term laser flicker noise of $5 \cdot 10^{-2}$%. Power

Table 2
Operating characteristics of the diode lasers used in this study

Diode laser (type)	Wavelength (nm)[a]	Maximum power (mW)	Operating current (mA)	Detection limit[b] (p*M*)
Philips CQL84/D	635	3	100	2 (1.5)
Toshiba TOLD 9410	650	3	80	0.7 (0.7)
Toshiba TOLD 9220	660	3	65	0.7 (0.7)
Toshiba TOLD 9211	670	5	55	0.3 (0.4)
Toshiba TOLD 9215	670	10	45	0.2 (0.3)

[a] Nominal values; characteristics never differed more than 1 nm from these values.
[b] Taken as $S/N = 3$ at maximum output power, 3 times determined; values obtained for the diode lasers in combination with the laser-line selector are given in parentheses.

stabilization is also useful because the power/current characteristics and thus the output intensity of diode lasers vary significantly with temperature.

A light-efficient Meredith AR coated multi-element LDC-10 lens (>85% transmission) was applied to collimate the diode laser beam in all cases. If required, excitation wavelength selection was performed with a laser line selector (Applied Photophysics, London, England).

Argon-ion laser

A Coherent (Palo Alto, CA, USA) Innova 200-10 argon-ion laser is used for the excitation of a Coherent CR-590 Rhodamine 101 dye laser. Laser light of the fundamental frequency and non-lasing plasma lines are rejected by quartz prisms and glass cut-off filters. The selected excitation frequency is 635 nm; a power of 100 mW is available at the flow cell.

3. Results and discussion

3.1 HeNe lasers

To examine the importance of Raman scatter in NIR LIF detection during methanol–water gradient elution, Raman spectra were recorded applying 633 nm excitation (see Fig. 3). It is clear that both the total intensity of the Raman scatter and the fraction detected within the filter bandpass is much larger for methanol than for water (3.5:1). The short-pass filter reduces the background at least four times, while diminishing the transmitted intensity of the emission from the model compound with only some 25%. A chromatogram recorded for $1 \cdot 10^{-11}$ *M* (10 p*M*) AlPcS2 using the 15 mW HeNe laser and applying the direct detection scheme, is depicted in Fig. 4. The gradual increase of the background with time can be fully attributed to Raman scatter, which increases 2-fold during the gradient run which starts at 25% and ends at 90% methanol.

The detection limits obtained with the HeNe lasers are 1 p*M* (2 mW laser) and 0.4 p*M* (15 mW laser) ($S/N = 3$, peak-to-peak noise). The 2.5-fold improvement realized when using the more powerful HeNe laser indicates that shot noise dominates. With photon counting instead of direct detection, essentially the same detection limits were obtained. The linear dynamic range extends to about $1 \cdot 10^{-8}$ *M* and can be further increased to $1 \cdot 10^{-6}$ *M* by utilizing neutral density filters to avoid PMT overloading.

3.2 Diode lasers

The detection limits obtained with the five diode lasers (Table 2) range from 0.2 to 2 p*M* and, as for the HeNe lasers, ratioing does not improve these values; the linear dynamic range extends from the detection limit to about $1 \cdot 10^{-8}$ *M*, similar to the HeNe lasers. The flicker noise contribution of the diode lasers is negligible, even with the LDD-200 driver.

Analogous to gas lasers, diode lasers provide

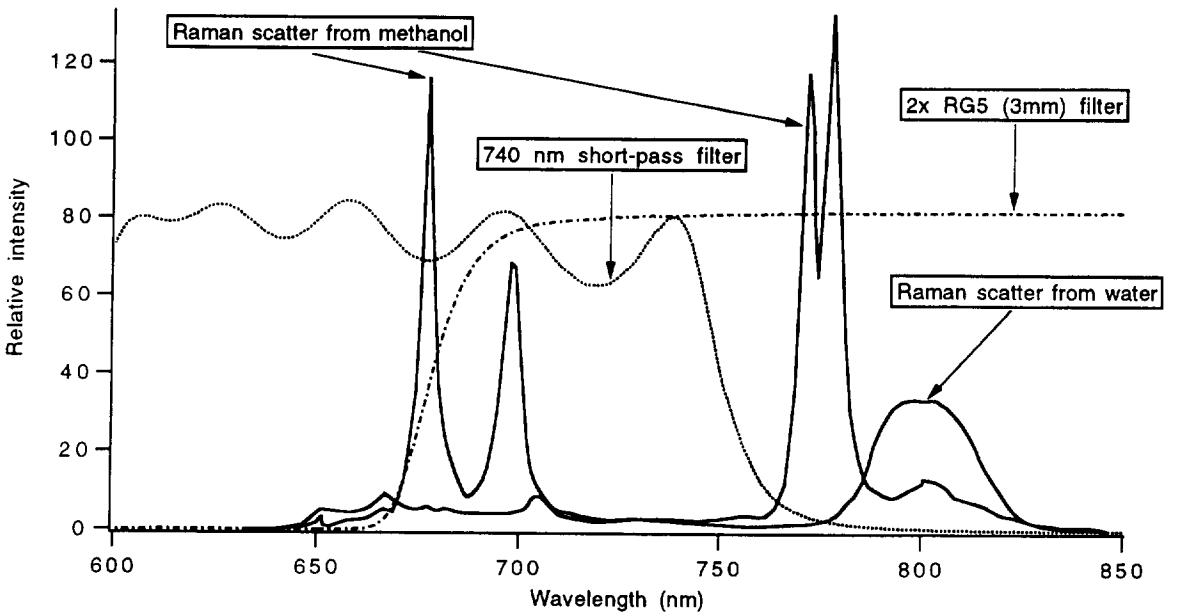

Fig. 3. Raman spectra of methanol and water (solid lines) and the relative transmittance of the applied filters for 633 nm excitation (dashed lines).

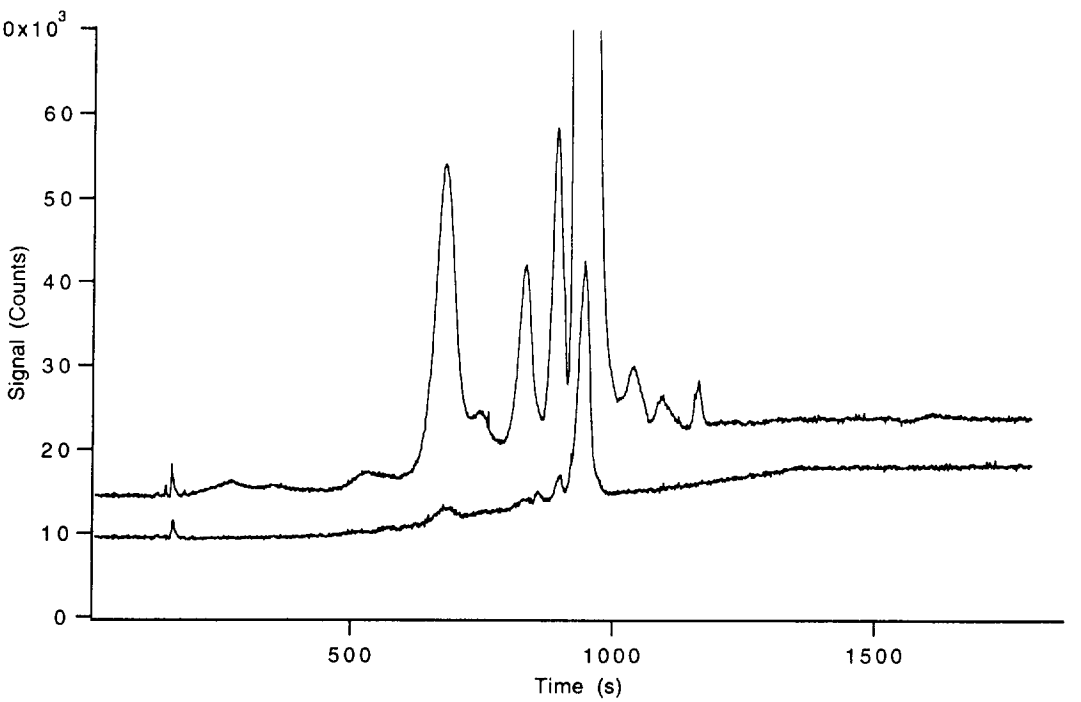

Fig. 4. Gradient LC chromatograms of 10 p*M* (lower trace) and 250 p*M* (upper trace) AlPcS2, recorded with the direct detection system using a 15 mW HeNe laser. For chromatographic conditions see Experimental.

spontaneous unpolarized emission in addition to laser light, which consists of a broad band, sometimes more than 100 nm wide (cf. ref. 14), and is often a major source of background. The higher the threshold current of the laser, the higher the fraction of non-lasing emission [14]. From Table 2 it is clear that especially the diode lasers emitting short-wavelength radiation have a high threshold current. Therefore, for these devices a laser line selector, which functions as a 2 nm bandpass filter (50% transmission; reducing the signal intensity 2-fold) around the lasing wavelength, was inserted in the excitation beam to remove spontaneous emission. Thus, the background is reduced up to 15-fold for the Philips CQL84/D at maximum operating current (see Fig. 5A). It is clear that except for the low-threshold TOLD 9215 in absence of the laser line selector, a large part of the background observed results from non-lasing emission (Fig. 5C). Nevertheless, in practice the improvement achieved by utilizing the laser line selector is only significant for the CQL84/D; see Table 2. Furthermore, the shot noise difference due to the 20 percent difference in Raman scatter at 635 nm and 670 nm is hardly detectable.

The repeatability of the alignment was checked by fivefold injection of $5 \cdot 10^{-11}$ *M* AlPcS2 on the same detection system. After each measurement the laser and the flow cell were taken from the optical bench and the fibers were removed from the flow cell. No more than 15% difference in *S/N* was found between any two of these measurements. Ten consecutive measurements without removing the fibers resulted in a R.S.D. of only 2.8%.

3.3 Argon-ion laser

When using direct current-to-voltage conversion of the PMT signal, the detection limit of AlPcS2 is 0.25 p*M* at 635 nm (100 mW), less than 2-fold better as obtained with the 15 mW HeNe laser.

Since for the argon-ion laser flicker noise contributions are significant, noise on the background increases faster during gradient elution than observed in Fig. 4. Using photon counting, the background at the start of the gradient was $(7.7 \pm 0.1) \cdot 10^4$ with a noise of $(1.9 \pm 0.1) \cdot 10^3$ counts and at the end of the run $(1.50 \pm 0.05) \cdot 10^5$ with a noise of $(3.1 \pm 0.15) \cdot 10^3$ counts. Ratioing enabled a reduction of the noise to $(1.20 \pm 0.06) \cdot 10^3$ and $(1.70 \pm 0.10) \cdot 10^3$ counts, respectively, and an improvement of the detection limit of AlPcS2 from 0.3 p*M* to 0.2 p*M*.

The flicker noise on the output power of the laser can be estimated using the above information and the fact that for the ratioing procedure a reference signal of $2.3 \cdot 10^6$ counts ($30\times$ the background signal at the start of the gradient) was used. After correction for the introduction of additional shot noise by the reference signal (0.25%), the flicker noise in the output intensity of the argon-ion laser can be calculated to be about 1%. Thus, at the beginning of the gradient the relative importances of shot and flicker noise is 0.8 to 1.1; at the end their contributions are equal, i.e. $1.5 \cdot 10^3$ counts.

Analog ratioing gives a 0.15 p*M* detection limit for AlPcS2, a marginal improvement compared to photon counting. For all argon-ion laser based detection systems described, the linear dynamic range extends from the detection limit to about $1 \cdot 10^{-8}$ *M*.

3.4 Comparison

Comparison of the detection limits obtained for the various CW lasers (0.4 p*M* for the 15 mW HeNe laser; 0.2 p*M* for the 10 mW diode laser and 0.15 p*M* for the 100 mW argon-ion laser) shows that, as expected under shot noise-limited conditions, the analyte detectability improves with the square root of the laser power. To show this dependence, corrections have to be made for the excitation efficiency of the model compound and the fluorescence collection efficiency through the emission filters used to remove scattered excitation light. To quote one example, when comparing the performances of the 100 mW 635 nm argon-ion laser and the 10 mW 670 nm diode laser, the improvement is $\sqrt{10}$-fold, since at 635 nm excitation is 4.5-fold less efficient, while the emission collection efficiency is 2.3 times higher. As a result, the detection limit at 635 nm should

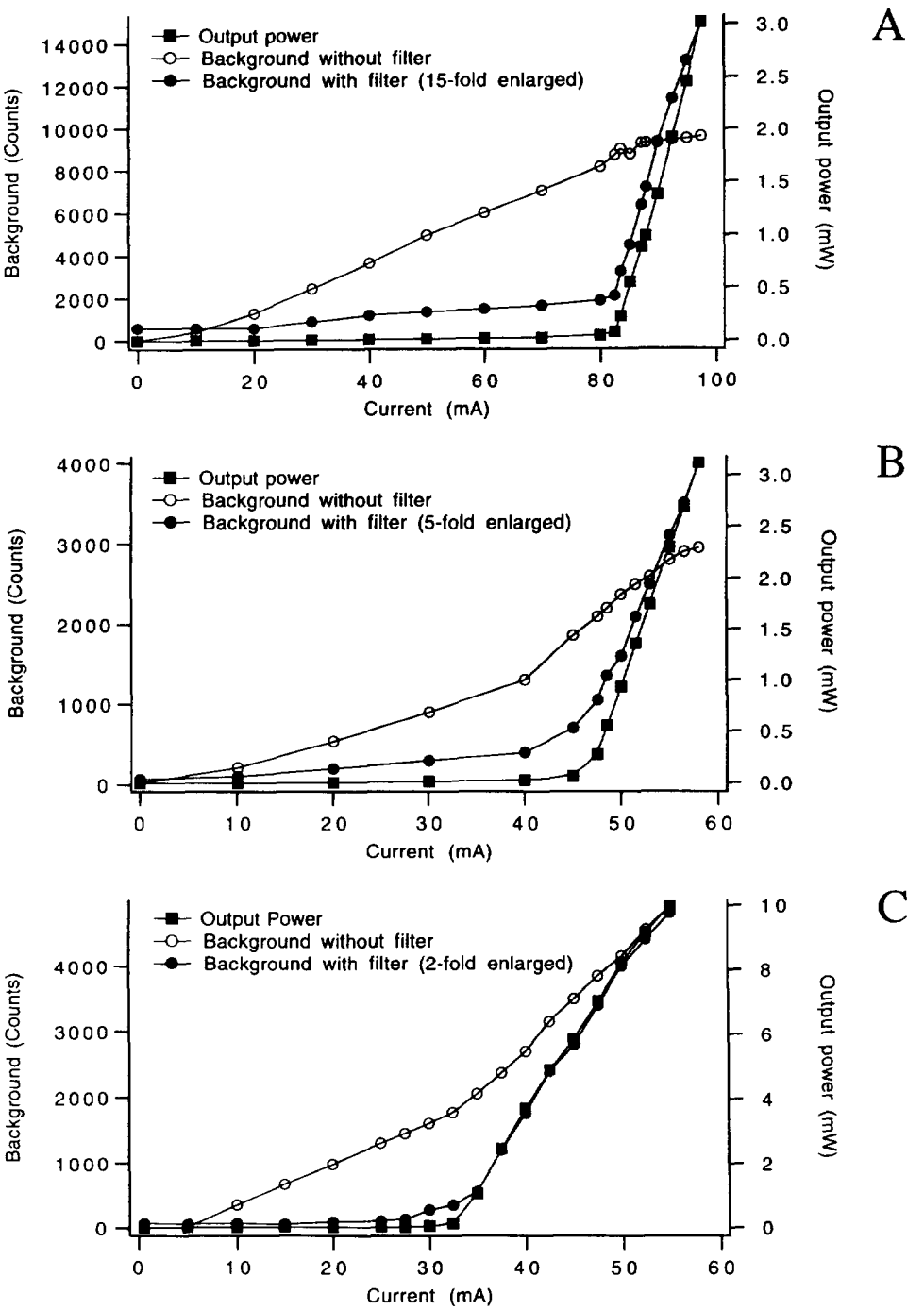

Fig. 5. Background (with and without laser line selector) and output power as a function of the current applied to the laser.

be about 1.5 times lower, provided the background remains the same, indeed very close to the observed ratio of 1.3.

After similar correction, the detection limits for the other CW lasers, including the different diode lasers, can also be explained by the differences in Raman scatter and excitation power if shot noise-limited conditions are assumed.

Since for both the HeNe and the diode lasers ratioing is not necessary, the second fiber in the flow cell can be used to detect the fluorescence signal, which effectively increases the emission collection efficiency 2-fold. Thus, similar detection limits were observed using the 10 mW diode laser and the argon-ion laser.

4. Conclusions

The present study shows that HeNe and diode lasers are appropriate excitation sources for NIR LIF detection in LC. They are by far the cheapest lasers available and due to their stability ratioing is not required; detection limits are better than 1 p*M* for AlPcS2 in standard solutions. Their lack of tunability is not a major disadvantage in LC detection. In view of the broad-band excitation spectra of analytes, in practice efficient excitation will be possible for a wide range of NIR-absorbing compounds by utilizing a number of diode lasers emitting at different wavelengths. More importantly, in everyday practice it will not often be possible to apply direct fluorescence detection in the NIR region; consequently, fluorescent tagging will be necessary in many cases [15] and the absorption wavelength of the label can be tailored to a wavelength available from a NIR emitting laser. A critical note should be made here. Although the detection of labelled compounds obviously can also be performed in the p*M* concentration range, derivatization of analytes at this concentration level is often not possible. Today it is increasingly being recognized that for analyte concentrations below 10^{-9} *M* problems are encountered either because reaction rates are not high enough or because side products and/or excess labelling reagent are present in the derivatization mixture. This implies that for detection after pre-column derivatization LIF detection in LC, the use of conventional lasers such as the argon-ion laser, can be considered an overkill. However, the use of cheap HeNe- and diode laser-based detection systems in combination with NIR-absorbing labels should prove to be a suitable alternative to existing labelling methods applicable at shorter wavelengths.

References

[1] J.M. Bostick, J.V. Strojek, T. Metcalf and T. Kuwana, *Appl. Spectrosc.*, 46 (1992) 1532.
[2] A.J.G. Mank, H. Lingeman and C. Gooijer, *Trends Anal. Chem.*, 11 (1992) 210.
[3] A.J.G. Mank, C. Gooijer, H. Lingeman, N.H. Velthorst and U.A.Th. Brinkman, *Proc. SPIE*, 2084 (1993) 255.
[4] J.W. Hofstraat, C. Gooijer and N.H. Velthorst, in G. Schulman (Editor), *Molecular Luminescence Spectroscopy Part 3*, (*Chemical Analysis Series*, Vol. 77), Wiley, NY, 1993, Ch. 9.
[5] A.J.G. Mank, C. Gooijer, H. Lingeman, U.A.Th. Brinkman and N.H. Velthorst, *Anal. Chim. Acta*, 290 (1994) 103.
[6] M. Ambroz, A. Beebey, A.J. MacRobert, M.S.C. Simpson, R.K. Svensen and D. Philips, *J. Photochem. Photobiol. B: Biol.*, 9 (1991) 87.
[7] R.K. Svensen, S. Fery-Forgues, A.J. MacRobert and D. Philips, in G. Moreno (Editor), *NATO ASI Series Vol. 15, Photosensitisation*, Springer, Berlin, 1988, p. 445.
[8] K. Lang, D.M. Wagnerová, P. Engst and P. Kubát, *J. Chem. Soc. Faraday Trans.*, 88 (1992) 677.
[9] A. Beeby, A.W. Parker, M.S.C. Simpson and D. Phillips, *J. Photochem. Photobiol. B.: Biol.*, 16 (1992) 73.
[10] V.R. Meyer, *J. Chromatogr.*, 334 (1985) 197.
[11] R.J. Fonck, R. Ashley, R. Durst, S.F. Paul and G. Renda, *Rev. Sci. Instrum.*, 63 (1992) 4924.
[12] H.V. Malmstadt, M.L. Franklin and G. Horlick, *Anal. Chem.*, 44 (1972) 63A.
[13] J.D. Ingle, Jr. and S.R. Crouch, *Spectrochemical Analysis*, Prentice Hall, Englewood Cliffs, NJ, 1988, p. 155.
[14] A.P. Larson, H. Ahlberg and S. Folestad, *Appl. Opt.*, 32 (1993) 794.
[15] A.J.G. Mank, E.J. Molenaar, H. Lingeman, C. Gooijer, U.A.Th. Brinkman and N.H. Velthorst, *Anal. Chem.*, 65 (1993) 2197.
[16] A.J.G. Mank, N.H. Velthorst, U.A.Th. Brinkman and C. Gooijer, *J. Chromatogr. A*, 695 (1995) 175.